34th Annual International Conference of the IEEE EMBS
San Diego, California USA, 28 August - 1 September, 2012

Artificial Tissue Bioreactor (ATB) for Biological and Imaging Applications

Timothy D. Whitehead, Samuel T. Nemanich, Kooresh I. Shoghi*

Abstract— **Three-dimensional (3D) culture systems are increasingly applied to study tissue biology. In this work, we report on the development of an artificial tissue bioreactor (ATB) designed to simulate the 3D structure and microenvironment of tissues in vivo, with multiple avenues of sampling, including the tissue chamber, for downstream analysis. Additionally, the ATB is integrated with the microPET Focus F220 for in-vivo imaging applications. As a proof-of-concept, we characterized the effects of lipids on glucose utilization using HepG2 cells. ATB studies were performed pre- and post- therapeutic intervention with the PPAR-γ agonist pioglitazone. In parallel, Glucose Tolerance Test (GTT) is performed on media samples to assess glucose uptake by cells as a measures of insulin signaling sensitivity. Fatty acid uptake in the ATB cell chamber is measured using [^{11}C]Palmitate with microPET imaging. Overall, the ATB will facilitate the use of existing and novel radiopharmaceuticals in discovery of validating and translating insights derived from ATB studies to pre-clinical animal studies, to clinical evaluation.**

I. Introduction

An artificial tissue bioreactor (ATB) is a versatile system designed to simulate the three-dimensional (3D) structure and microenvironment of tissues in vivo. It offers an environment in which biological processes are closely controlled and monitored (pH, temperature, pressure, nutrient supply, waste removal, and stress) by design[1]. In doing so, ATBs offer a platform for research and discovery by allowing manipulation of specific tissue processes under controlled conditions to elucidate tissue-specific disease mechanisms for therapeutic and imaging biomarkers thereof. In this work, we present preliminary studies on the development of an ATB and its integration with the microPET Focus F220.

II. Materials and Methods

A. System Description

A schematic diagram of the bioreactor system is shown in Fig. 1. The cell chamber is in a circulating perfusion path powered by a peristaltic pump, a gas exchanger, septum for bolus injection, and another vessel needed to degas the system during filling and priming. Dissolved oxygen (DO) probes with temperature sensors are located at the inlet and outlet of the cell chamber and a pH probe is located at the chamber outlet. Fresh media is pumped continuously into the bioreactor near the outlet of the degas vessel, is circulated through the system, and the effluent is collected in the fraction collector as 'mixed cup' samples that can be stored for later analyses, or is directed to waste.

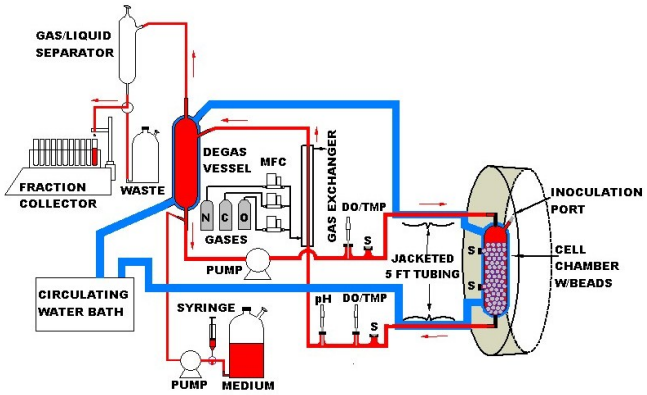

Figure 1. Schematic diagram of ATB system. . See text for description. MFC-mass flow controllers, S-septa, DO/TMP- combined dissolved O2 & temperature probe

The cell chamber is a custom blown, water-jacketed, glass vessel containing borosilicate glass beads between 1.4 and 1.7 mm diameter (between 14 and 12 mesh) with a measured void space of 40%. Septa ports are located along the length of the chamber for obtaining cell samples for western blots, microarray assays, etc., during the experiment. A platform designed to fit in the microPET® Focus F220 scanner holds the cell chamber and the probes proximal to the chamber inlet and outlets.

Bolus, step-pulse, and constant composition are the three general input functions for the bioreactor. A bolus of tracer, drug, metabolic substrate, etc. is injected through the inline septum located upstream of the gas exchanger and mixing bottle. A pulse-step input function is achieved using the syringe upstream of the input pump. A concentrate of the compound in media sufficient to achieve the desired C_{max} is placed in the syringe. A stopcock is used to divert flow from the media bottle to the syringe at time 0, and back again when the sample delivery is completed. A constant composition input function is achieved by adding (or removing) the compound or metabolic substrate to the media feed at the desired concentration.

The effluent is collected continuously as "mixed cup" samples in the fraction collector, which sends a signal to the

*Research supported by internal funding from the Mallinckrodt Institute of Radiology (MIR) and partly by NIH/NIDDK award 5R01DK085298.

T. D. Whitehead, S. T. Nemanich, and K. I. Shoghi are with the Mallinckrodt Institute of Radiology (MIR), Division of Radiological Sciences, Saint Louis, MO, 63110. For correspondence, contact shoghik@wustl.edu.

computer for time stamping with each tube change. Because the recycle perfusion flow rate is about 100 times greater than the feed input flow rate, the effluent concentration profile is identical to that of a perfectly mixed tank, and the average residence time is equal to the reactor volume/input flow rate. Therefore, metabolic or production rates, or tracer concentration curves based on effluent sample analyses can be readily calculated using the constant stirred tank reactor model (CSTR).

System control consists of an Instrunet network control board (inet-PCI200) installed in a Dell Optiplex 780 computer with Intel duo Core 2 processor, and an A/D I/0 network terminal connector (inet-100HC). DASYLab (National Instruments, Austin, TX) software is used to develop the data acquisition and process control.

B. Experimental ATB Studies

As proof-of-principle, we designed an ATB study to investigate the effects of lipids on glucose utilization in HepG2 (ATCC, Manassas, VA) cells at various time points in the intervention. In addition, the therapeutic response was assessed with the addition of pioglitazone, a PPARγ agonist, which is known to stimulate glucose utilization. Finally, a PET imaging study was performed to assess response of the system in-vivo.

Dulbecco's modified Eagle's Medium (DMEM) without glucose, pyruvate, L-glutamine, phenol red, or bicarbonate, (D5030, Sigma, St. Louis, MO) was used throughout the experiment to allow modification of the feed composition as needed. The media powder and 3.9 gm of sodium bicarbonate were dissolved in 900 mL deionized water and filter sterilized. To this media was added 100 mL of fetal bovine serum (FBS, Atlanta Biological, Lawrenceville, GA), 2 mM L-glutamine and 1 mM sodium pyruvate (Cellgro, Manassas, VA)), 100 IU/mL penicillin, 100 µg/mL streptomycin (Invitrogen, Carlsbad, CA), and 2 ng/mL insulin (Sigma). When the protocol required, free fatty acid (FFA) concentrate (Invitrogen, Carlsbad, CA) was added to a final concentration of 100 µmol/liter, and pioglitazone (Sigma) in dimethyl sulfoxide (10 mg/mL) was added to a final concentration of 1.0 µg/mL. The glucose concentration was adjusted according to protocol.

HepG2 cells were maintained in DMEM with 100 mg/dL glucose (normal glucose) in a 37°C, 5% CO_2, humidified incubator. The cells were expanded for inoculation under the same conditions in 3-layer T175 flasks. The cells from all flasks were trypsinized, combined, and rinsed and centrifuged. The cell pellet was suspended in fresh media, and three 2 mL samples were passed through 40 µm cell strainers. The cell concentration (Coulter Counter Z2, Beckman-Coulter) and packed cell volume per unit volume of media (PCV tubes, Midwest Scientific) were measured to calculate the specific packed volume of the hepatocytes. The packed volume of the remaining cells was determined by centrifugation in a graduated tube. The pellet was suspended in 5 mL of fresh media, drawn into a syringe and injected into the bioreactor. The total cell count injected was approximately 3.5×10^8 cells.

After the cells had aggregated and settled into the bead matrix (~16 hours), feed media with 100 mg/dL glucose was started with a constant flow rate of 0.5 mL/min. Effluent samples of approximately 5 mL were collected every hour, except where noted. The cell mass was allowed to expand for 5 days before the first glucose tolerance test (GTT).

The glucose concentration was reduced to 25 mg/dL (low glucose) in the feed media approximately 20 hours prior to bolus glucose dosing to simulate fasting conditions. A bolus of glucose concentrate calculated to achieve a C_{max} of 300 mg/dL (no cell condition) was injected. Input media flow was uninterrupted during the GTT and was of the same composition as fasting condition media (low glucose).

Sample collection was increased to once every 10 minutes for the first hour, then returned to normal rate thereafter. After the 24 hour GTT, the input media flow was returned to normal glucose levels. The glucose concentration measured on the effluent samples were used to evaluate glucose uptake. GTT were performed on the cells prior to lipid exposure, after lipid exposure, and after lipid exposure and treatment with pioglitazone (PGZ) for 3 days at 1µg/mL. PGZ (a 15-45 mg tablet results in 0.5-1.0 µg/mL blood C_{max}) has been shown to reduce fat accumulation and improve insulin sensitivity in liver [2, 3] A timeline of the experiment and its conditions is shown in Table 1 (the letter next to the event description is used to identify the event on subsequent figures).

TABLE I. EXPERIMENT TIMELINE (hours post inoculation)

Time (h)	Event	Input Media Substrate and Drug Composition
17	A. Expand cells	Normal glucose[a]
120	B. Fast	Low glucose[b]
138	C. GTT	Low glucose
162	D. Expand cells	Normal glucose + lipid[c]
237	E. Fast	Low glucose + lipid
258	F. GTT	Low glucose + lipid
286	G. Expand cells	Normal glucose + lipid + PGZ[d]
334	H. Fast	Low glucose + lipid + PGZ
358	I. GTT	Low glucose + lipid + PGZ
520	PET imaging #1	Low glucose + lipid
643	PET imaging #2	Low glucose

[a][Glucose]=100 mg/dL; [b][Glucose]=25 mg/dL; [c]Total [lipid]=100 µmol/L;[d][PGZ]=1 µg/mL

C. PET protocol

Two imaging studies were performed after the GTTs. During the first, lipid concentrate was still available in the feed media. After this, lipid was removed and another imaging session was conducted three days later.

The PET protocol was as follows: 20 minute transmission scan followed by a 45 minute [^{11}C]Palmitate (0.75-1.0 mCi) scan. Cells were fasted (low glucose) 24 hours prior to

imaging and input flow rate was increased to 5 mL/min to ensure clearance of tracer and metabolites. Manual samples (10-30 µL) were drawn from the input and output of the cell chamber and corrected for ^{11}C metabolites for input function estimation. For comparison with manual samples, effluent samples were also collected every minute.

D. Analyses of ATB Data

Effluent samples were assayed for glucose and lactate concentrations (Sigma glucose and lactate kits) in duplicate, and packed cell volume (PCV) of effluent samples was measured to determine cell losses during the experiment. The area under the curve (AUC) of each GTT was calculated as a measure of extent of glucose uptake.

Regions of interest (ROI) were drawn on reconstructed PET images of the ATB in various regions to show heterogeneity. Time-activity curves (TAC) were then normalized based on the injected activity to give a standard uptake value (SUV).

III. Results

A. Cell substrate and microenvironment

The dissolved O_2, DO, at the inlet and outlet of the cell chamber are plotted in Fig. 2 along with the calculated consumption rate. The primary factor affecting O_2 consumption rate is cell number. Therefore, it is the primary method for monitoring the cell growth progression and death (effluent cell debris volume also monitors cell death). The consumption rate, and possibly cell growth, appears to have reached a steady state at about 320 hours.

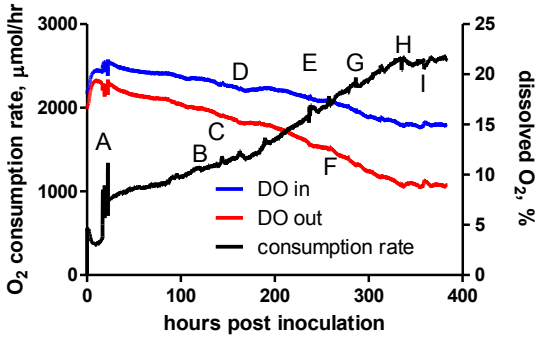

Figure 2. Dissolved oxygen and O_2 consumption time course.

The effluent glucose and lactate consumption and production rates over the experiment duration are shown in Fig. 3. During the inoculation and seeding period there is no fresh media flow into the bioreactor so that the glucose concentration drops substantially and the lactate accumulates. When feed is started the glucose level rises and the excess accumulated lactate is flushed from the system (data not shown). An interesting observation is that the rates of both O_2 consumption and lactate formation increase with the introduction of lipid. This observation suggests that the cells favored fatty acid and diverted glucose metabolism toward the glycolytic pathway.

Intracellular concentrations of FFA and triglyceride, TG, (data not shown) over the course of the experiment are consistent with feed media composition. There was an increase in both TG and FFA levels after lipid was introduced (event D to E) corresponding to increased concentration of lipid in the feed media. Following the glucose fast (event E to F), there was a decrease in both FFA and TG, indicating increased lipolysis due to lack of glucose availability. Lipid began to accumulate in the cells during the GTT (event F to G). The effect of the drug pioglitazone was seen during events G-I. There was an increase in TG during drug administration showing no drug action. However, rather than increasing as during the second GTT (event F-G), there was a net decrease in FFA and TG levels during the third GTT (event I), suggesting increased lipolysis in the presence of glucose and thus showing the effect of pioglitazone to reduce fatty acid esterification.

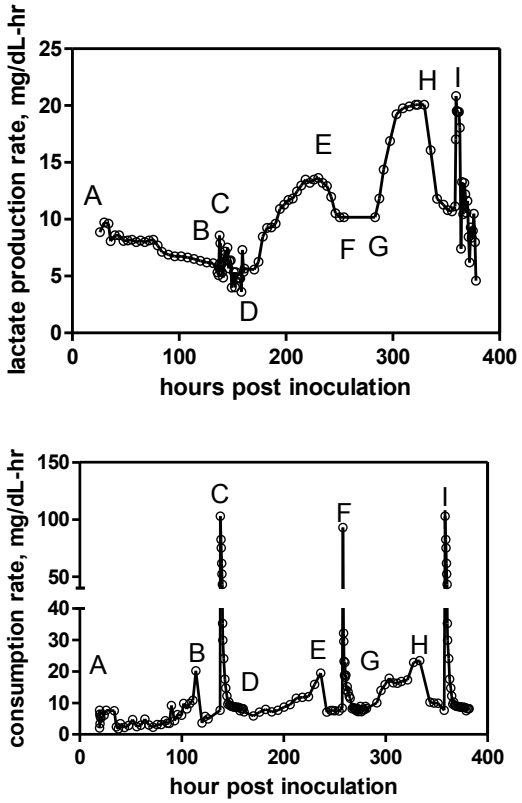

Figure 3. Lactate production rate (top) and glucose consumption rate (bottom). Lactate in the feed is from the FBS, which is constant throughout experiment. Capital letters near the curves match events in Table 1.

B. Glucose Tolerance Test (GTT)

The AUC of a GTT is a measure of glucose clearance from tissue. High AUC implies reduced uptake by tissue and increased glucose levels in the blood, or in this case, the media. Fig. 4 shows greater AUC in the presence of lipid compared to no lipid. After only two days of treatment, PGZ induced glucose uptake.

C. PET Imaging

One main advantage of the ATB is its integration with the Focus F220 small animal PET scanner. Fig. 5 shows an example summed PET image of [^{11}C]Palmitate with SUV

TACs, one with and one without addition of lipids. There are clear differences in the kinetics between the two regions R1 and R2 (Fig 5B), showing heterogeneity of cell expansion in the chamber. Furthermore, the input TAC (Fig 5C) does not vary between the imaging sessions. Finally, the SUV tissue plot (Fig 5C) shows higher uptake of [^{11}C]Palmitate when lipid was present in the feed media than when lipid was absent.

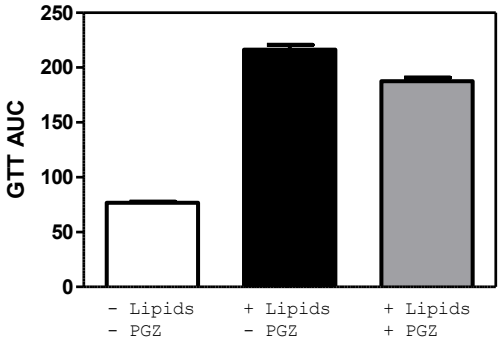

Figure 4. AUC of GTT under conditions of no lipid (open bar), addition of lipid (solid bar), and lipid + Pioglitazaone (gray bar). Error bars are one SD of glucose measurements. AUC was normalized to baseline glucose in each study.

IV. Discussion

In this feasibility study, we characterized the effects of lipids on glucose sensitivity and the therapeutic efficacy of the PPARγ agonist PGZ on glucose and lipid metabolism using an ATB with HepG2 human carcinoma cells. The ATB facilitated monitoring and control of the microenvironment throughout the ATB study. In parallel, we performed GTT, a common practice in both pre-clinical and clinical studies, to assess insulin sensitivity at various intervention time points in the ATB study. Finally, the integrated ATB with the microPET Focus F220 allows for "in-vivo" characterization of metabolism.

The introduction of lipid to feed media drastically decreased the glucose uptake (clearance from media) as measured by a GTT. On the other hand, PGZ acted to increase glucose uptake in the presence of lipid after only 3 days of treatment. PET imaging studies showed increased uptake of [^{11}C]Palmitate with lipid present in the media compared to lipid-free, consistent with observations of triglyceride droplet formation in HepG2 cells (data not shown). Following intervention with PGZ, we observed a modest clearance of glucose from the media as evident by a decrease in GTT values, suggesting that PGZ improved insulin sensitivity. Throughout the study, there was a net consumption of oxygen suggesting continuous growth of cells.

V. Conclusion

We have outlined an ATB system that has the capability to study cell population for prolonged periods, while ease of providing interventions and monitoring biological process. The integration of the system with the Focus F220 microPET scanner further allows for possible therapeutic and imaging biomarker discovery and validation for translational studies.

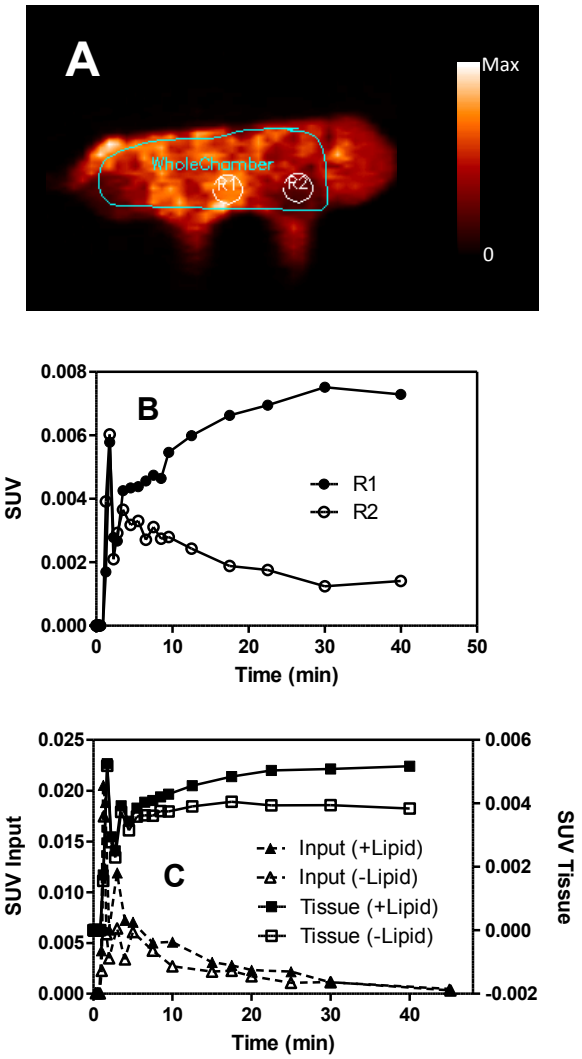

Figure 5. PET imaging study. (A) A sample image depicting heterogeneity of [^{11}C]Palmitate uptake. (B) Differences of kinetics of [^{11}C]Palmitate in regions of high and low uptake. (C) [^{11}C]Palmitate kinetics for input and chamber with and without lipid and the media.

Acknowledgment

The authors thank the small animal imaging facility at MIR for technical assistance and the cyclotron facility for synthesis of radiopharmaceuticals.

References

[1] I. Martin, D. Wendt, and M. Heberer, "The role of bioreactors in tissue engineering," *Trends Biotechnol,* vol. 22, pp. 80-6, Feb 2004.

[2] M. L. Christensen, B. Meibohm, E. V. Capparelli, P. Velasquez-Mieyer, G. A. Burghen, and W. V. Tamborlane, "Single- and multiple-dose pharmacokinetics of pioglitazone in adolescents with type 2 diabetes," *J Clin Pharmacol,* vol. 45, pp. 1137-44, Oct 2005.

[3] H. Yki-Jarvinen, "Thiazolidinediones and the liver in humans," *Curr Opin Lipidol,* vol. 20, pp. 477-83, Dec 2009.